

Development of permeability properties of polyamide thin film composite nanofiltration membrane by using the dimethyl sulfoxide additive

Ahmad Akbari and Sayed Majid Mojallali Rostami

ABSTRACT

A novel polyamide thin film composite (PATFC) as a nanofiltration (NF) membrane was prepared by a modified interfacial polymerization (IP) reaction. Herein trimesoyl chloride and piperazine as the reagents, dimethyl sulfoxide (DMSO) as additive and polysulfone (PSF) ultrafiltration membrane as support were used respectively. The main goal of the present study is to improve TFC membrane water flux by addition of DMSO into the aqueous phase of IP reaction, without considerable rejection loss. Morphological, roughness, and chemical structures of the PATFC membrane were analyzed by scanning electron microscopy, atomic force microscopy (AFM), and Fourier transform infrared spectroscopy (FT-IR), respectively. The AFM analysis demonstrated that as DMSO was added to the aqueous phase, the surface roughness of PATFC membrane increased. Results showed that the pure water flux of modified-PATFC membranes increased up to 46%, compared to nonmodified-PATFC membrane, while salt rejection was not sacrificed considerably. The results elucidated that the addition of DMSO leads to an increase in the number of cross-linking bonds between monomers and pore diameter, which results in enhancement of the membrane flux. Finally, the results showed that the newly developed PATFC membrane is a high-performance NF membrane which augments the efficiency of conventional PATFC membrane.

Key words | DMSO additive, interfacial polymerization, nanofiltration, PATFC, PSF

Ahmad Akbari (corresponding author)

Sayed Majid Mojallali Rostami

Institute of Nanoscience and Nanotechnology,

University of Kashan,

Kashan,

I. R. Iran

E-mail: Akbari@kashanu.ac.ir

INTRODUCTION

Nanofiltration (NF) is a relatively new membrane separation technique, which was developed in the 1980s based on reverse osmosis (Chiang *et al.* 2009). Based on the performance of NF membrane, it is a kind of pressure-driven process between reverse osmosis and ultrafiltration processes. NF membranes have several advantages, such as high flux, high retention of multivalent salts, low operating pressure, low primary investment and operating costs (Jahanshahi *et al.* 2010; Rahimpour *et al.* 2010). This technology is rapidly growing for different applications, such as heavy metals' treatment (Ahmad & Ooi 2006; Bouranene *et al.* 2008), water softening (Uyak *et al.* 2008), color removal (Chakrabarty *et al.* 2003), separation textile dye (Akbari *et al.* 2002, 2006), chemical oxygen demand, and biological oxygen demand reduction (Chakrabarty *et al.* 2003; Lopes *et al.* 2005). Recently, NF membranes have also been studied for

applications in food and bio-process purposes (Manttari *et al.* 2006).

A key advantage of the thin film composite (TFC) membrane approach is that the materials for porous sublayers and top skin layer can be chosen separately to achieve the best overall separation and membrane stability (Petersen 1993; Rahimpour *et al.* 2010).

Surface modification has commonly been used to improve membrane performance of prepared membranes. There are several techniques for preparation of TFC membranes, such as plasma-initiated polymerization, photo-initiated polymerization, photo-grafting, electron-beam irradiations, dip-coating, and interfacial polymerization (IP) (Mulder 1996; Wei *et al.* 2008). Among these, the IP method is commonly used for preparation of composite membrane. In this technique, a thin film is generated by forming an ultra-thin top layer upon a

porous substrate. In the IP method, reactive monomers (usually diamine and acid chloride) are dissolved in two immiscible phases, and the IP of the reactive monomers occurs on the surface of the porous support membrane (Korikov *et al.* 2006; Verissimo *et al.* 2006). IP reaction takes place at the interface of two phases, because water and the hydrocarbon solvent are immiscible (Abu Seman *et al.* 2011). Development of solvent resistant, antifouling resistant, thermally stable, selective and permeable membranes in NF has received much interest in recent years (Mukherjee *et al.* 1994; Hirose *et al.* 1996; Belfer *et al.* 2001).

In the presence of additives such as alcohols (propanol or isopropanol), ethers, sulfur compounds, and monohydric aromatic compounds, the prepared aromatic polyamide thin film composite (PATFC) membrane shows superior water flux and reasonable salt rejection characteristics (Kwak *et al.* 2001; Kim *et al.* 2005). Application of additive during IP reduced the solubility difference and lowered the interfacial tension, which facilitated the diffusion rate of amine molecules to the organic phase (Hirose *et al.* 1997; Kim *et al.* 2005).

The purpose of the current study is to investigate the role of dimethyl sulfoxide (DMSO) as an additive in the IP which leads to preparation of a high-performance PATFC NF membrane through the solubility expansion. PATFC membrane was prepared by IP of piperazine (PIP) and trimesoyl chloride (TMC) in the presence of triethylamine (TEA) and addition of different amounts of DMSO into the aqueous phase, on the support surface (PSF ultrafiltration membrane, 600 L/m².h.bar). The morphological, topological and chemical characteristics of the resulting membranes were studied by scanning electron microscopy (SEM), atomic force microscopy (AFM), and Fourier transform infrared spectroscopy (FT-IR), respectively. Finally, the performance of PATFC NF membranes were characterized using filtration separation of aqueous feed solutions containing NaCl, Na₂SO₄, and MgSO₄, and the relationship between salt rejection, water flux, and DMSO additive was discussed.

EXPERIMENTAL

Materials

The polysulfone Udel P-1700 (Mn: 17,000 gmole⁻¹, Aldrich Co., USA), 1,3,5-Benzenetricarbonyl trichloride (TMC,

Merck Co., Germany), piperazine (PIP, Merck Co., Germany), triethylamine (TEA, Merck Co., Germany), N-methyl-2-pyrrolidinon (NMP, Merck Co., Germany), polyethylene glycol (PEG, M.W. = 1,000, 1,500, 2,000, 4,000 and 6,000, Merck Co., Germany), n-hexane (Merck Co., Germany) and dimethyl sulfoxide (DMSO, Merck Co., Germany) were used as received without further purification.

Preparation of PSF membrane support

Polysulfone casting solution was prepared by dissolving 18 wt.% polysulfone in N-methyl-2-pyrrolidinon solvent with 11 wt.% PEG as the pore-former through stirring for 24 h at 70 °C. The stirring was carried out at 500 rpm. After formation of homogeneous solution, dope solution was held at the ambient temperature for 2 h to remove the air bubbles. The solutions were cast uniformly onto a glass substrate by a hand-casting knife with a knife gap set at 200 µm and then immersed in a coagulation water bath for at least 24 h until most of the solvent and water soluble polymer were removed (Chakrabarty *et al.* 2008).

Preparation of PATFC NF membranes

The preparation process of PATFC membrane is as follows. First, the support layer was immediately dipped into an aqueous diamine solution containing 2 wt.% piperazine, 0.4 (wt.%) TEA and different amounts of DMSO (0, 2, 4, 6, 8, and 10, wt.%) for 2 min at ambient temperature. Using a rubber roller excess solution was drained from the dip coated support membrane surface until no liquids remained. Subsequently, the PSF support membrane was clamped between two teflon frames with a 1 cm high and 4 cm × 8 cm inner cavity. Then, the organic solution of TMC (0.1 w/v.% in n-hexane) was poured into the frame where the conventional IP reaction occurred for 1 min. These membranes were thoroughly washed and stored in deionized water before evaluation studies.

Morphology, roughness, and chemical structure

Membranes surface and cross-sectional morphologies were obtained by SEM (SEM KYKY-EM 3200, China).

Membrane surface roughness was studied by atomic force microscopy (AFM, Scanning Probe Microscope, model NanoScope E). FT-IR (IBB-Bomem MB-100, Canada) was used to characterize the presence of specific functional groups on the PATFC membrane surfaces.

Membrane characterization

TFC NF membranes were characterized by measurement of pure water flux, salt rejection of monovalent (NaCl) and multivalent salts (Na_2SO_4 , MgSO_4) with total concentration of 2,000 ppm (2 g/l). The performances of the prepared membranes were analyzed using a batch cross-flow system. The effective membrane area was 21 cm^2 , and each membrane was subjected to pre-treatment pressure at 4 bar for 1 hour before the permeation experiments. The permeation tests were carried out under ambient condition with the temperature within $25 \pm 1^\circ\text{C}$ and 3 bar pressure. Rejection and permeability were calculated using the following equations (Zhang *et al.* 2006):

$$\text{Rejection}(\%) = \left[1 - \frac{C_p}{C_f} \right] \times 100$$

$$\text{Permeability} = \frac{\Delta v}{t.p.s}$$

where C_p (mg/l) is the permeate concentration, C_f (mg/l) is the feed concentration, Δv is the permeate volume (L), t is the permeation time (h), p is the operation pressure (bar),

and s is the effective membrane area (m^2). Concentrations of the salts were obtained through measurements of the conductivity of the aqueous solution using a conductometer (WTW, inoLab Cond 720 series, Germany).

Molecular weight cut-off (MWCO) of PATFC membrane with (6 wt.%) and without DMSO additive was investigated using different molecular weight of PEG molecules. The permeates and the feed solutions of PEG aqueous solutions were analyzed using UV-Vis spectrophotometer (GBC, model Cintra 101, Australia). The effect of pH on membrane charges and performance in basic (pH 11) and acidic (pH 3) condition was investigated.

RESULTS AND DISCUSSION

Membrane physicochemical characteristics

Figure 1 shows the surface and cross-section SEM images of PSF support and aromatic PATFC membranes with and without addition of DMSO. Figure 1(a) illustrates the smooth and integrity surface of PSF support and Figure 1(d) represents the top layer and finger-like structure of PSF support before formation of PA skin layer. The variation of the surface morphologies confirmed that the surface of the PSF membrane became uneven, and the PA skin layer was formed after IP reaction (Figures 1(b) and 1(c)). The formation of this skin layer is the key factor for performance of TFC membranes. Although cross-section morphology does not apparently show the pronounced difference between PA skin layer

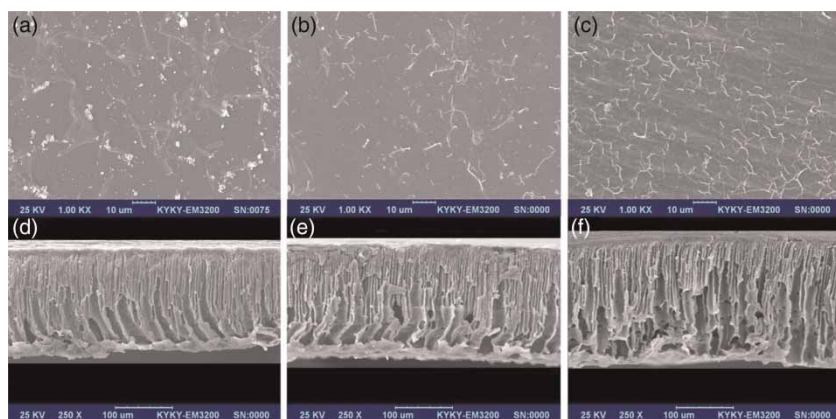


Figure 1 | Surface and cross-section SEM images of (a), (d) PSF support membrane, (b), (e) PA skin layer, (c), (f) PA skin layer in presence of 6 (wt.%) DMSO as additive.

with and without addition of DMSO (Figures 1(e) and 1(f)), Figures 1(b) and 1(c) show that the surface roughness of PA layer is increased in the presence of DMSO as additive. This could be evaluated by testing the performance of support membrane (PSF), which demonstrated nearly 0% rejection for Na_2SO_4 and a flux about $650 \text{ L.m}^{-2}.\text{h}^{-1}.\text{bar}^{-1}$, while the PATFC membrane shows nearly 96% rejection for Na_2SO_4 and a flux about $8.3 \text{ L.m}^{-2}.\text{h}^{-1}.\text{bar}^{-1}$.

Figure 2 illustrates the AFM images of the surfaces of PSF support and PATFC NF membranes over a scan area

of $5 \mu\text{m} \times 5 \mu\text{m}$. The surface roughness parameters of the membranes are presented in Table 1, which are expressed in terms of the mean roughness (S_a), the root mean square of the Z data (S_q). The mean difference between the highest peaks and lowest valleys (S_z) were calculated by AFM images and Nanoscope software.

The surface seems to be rougher with IP of PIP and TMC and formation of PA skin layer onto the PSF membrane surface which is due to the ability of PIP-TMC reactants to form a three-dimensional cross-linked structure on the

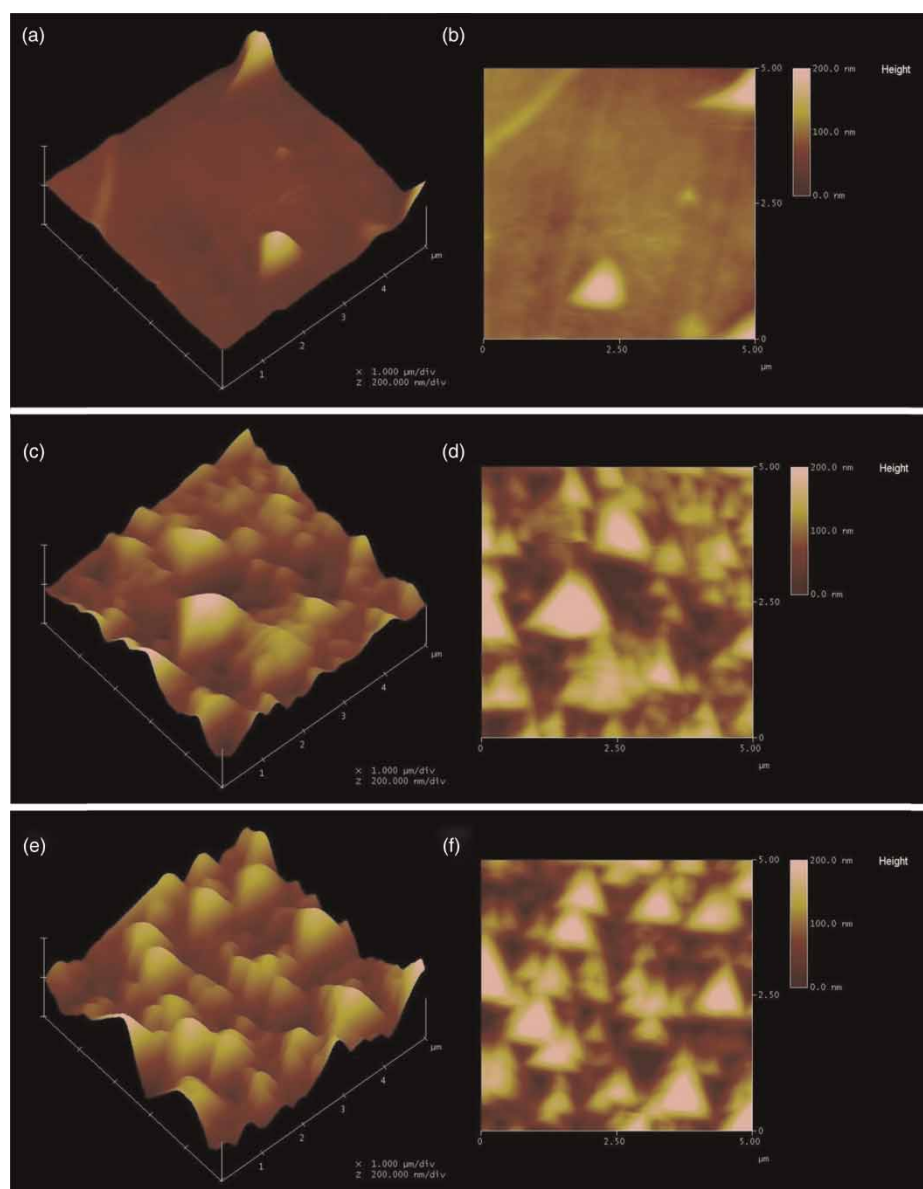


Figure 2 | Surface AFM images of PSF support membrane (a), (b), PATFC membrane without (c), (d), and in presence 6 wt.% DMSO as additive (e), (f).

Table 1 | Surface roughness parameters of PSF support, PATFC membrane without and in the presence of 6 wt.% DMSO

Membrane	Roughness		
	S_a (nm)	S_q (nm)	S_z (nm)
PSf support	10.261	17.147	177.89
PATFC	29.373	38.179	216.29
PATFC in presence of DMSO	39.310	45.923	354.85

surface of PSF membrane and an increase in roughness. Furthermore, the results of AFM images confirmed that the surface roughness of the PATFC membrane increases with addition of DMSO as additive to the aqueous phase.

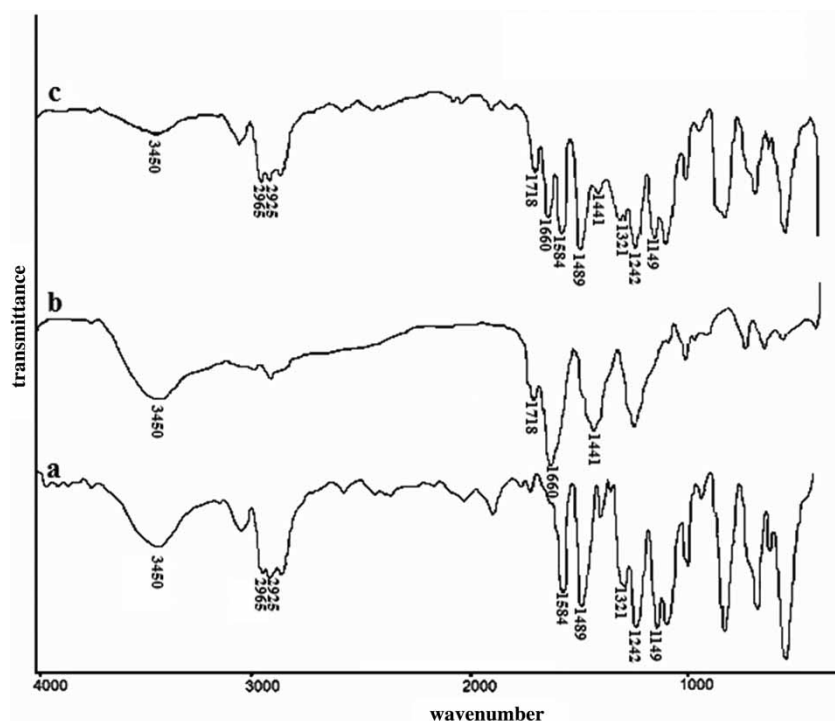
Figure 3 shows the FT-IR spectra of PSF support membrane, bare PA skin layer and PATFC membrane. The spectra of PSF support membrane displays peaks at around 2,965, 1,584, 1,489, 1,321, 1,242, and 1,149 cm^{-1} , which are the characteristics of PSF (Singh *et al.* 2006). The peaks at 2,965 and 2,925 cm^{-1} are assigned to the stretching vibration of C—H aliphatic, also bonds around 1,584 and 1,489 cm^{-1} belong to C=C in aromatic rings. The symmetric and asymmetric stretching vibration of S=O bonds appeared in 1,323 and 1,149 cm^{-1} . In addition,

the peak at 1,242 cm^{-1} was associated with the C—O—C stretching vibration in the PSF structure.

The characteristic hydroxyl peak, which appears at around 3,450 cm^{-1} , is due to the partial presence of PEG. This indicates that a few percent of PEG remain in the membrane matrix after precipitation (Puro *et al.* 2006).

The characteristics of the bare PA layer can be found in FT-IR spectra. The weak bond at 3,450 cm^{-1} is due to O-H stretching vibration of the carboxylic group. Two weak bands at 1,718 and 1,660 cm^{-1} are assigned to C=O stretching vibration of acid carboxylic and amide groups, respectively. The peaks at 1,441 cm^{-1} are assigned to C—N stretching bond. The traces of PSF membrane and PA skin layer can be found in the spectra of PATFC membrane. The FT-IR spectra confirm that the IP of PA was successfully done on the surface of PSF support membrane.

Filtration experiments were performed using NaCl, Na_2SO_4 and MgSO_4 (total concentration of salts 2,000 ppm) as feed solutions. The effect of variation in DMSO concentration on pure water flux and salt rejection is shown in Figure 4. The addition of DMSO led to enhancement of the water flux of PATFC membrane without any considerable

**Figure 3** | FT-IR spectra of PSF support membrane, bare PA skin layer and PATFC membrane.

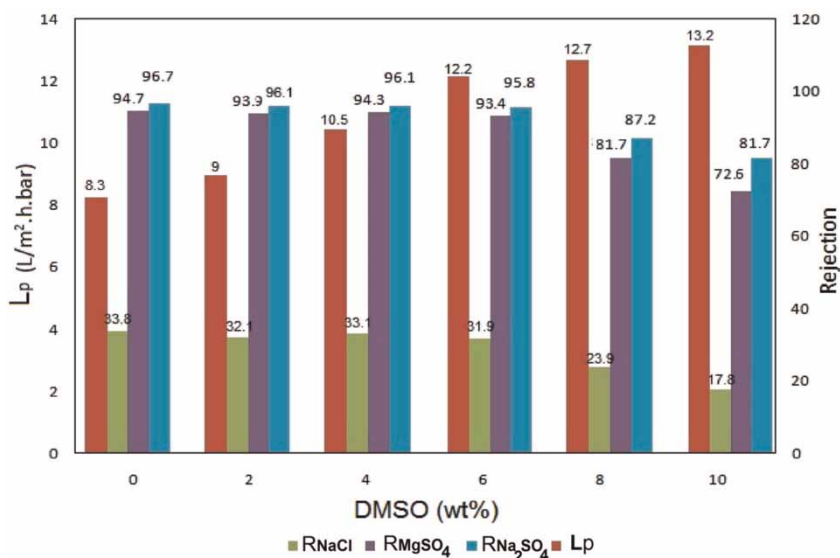


Figure 4 | Effect of DMSO additive content on pure water flux and rejection; concentration of 2,000 ppm NaCl, Na₂SO₄, and MgSO₄; operating pressure of 3 bar.

rejection loss. In the presence of 6% DMSO additive PATFC membrane shows higher water flux, up to 46%, in comparison with the PATFC membrane without DMSO additive.

In particular, PATFC membranes are prepared by IP of PIP and TMC in aqueous and organic phases. The IP reaction rates are immeasurably fast, and TMC is insoluble in water. Thus, the film growth rate is determined by the diffusion rates of monomers, especially in the diffusion rate of diamines to organic phase. Solubility parameter of water, n-hexane, and DMSO are 23.4, 7.3, and 12.2 (cal/cm³)^{1/2}, respectively. In fact, DMSO addition increases the miscibility between the aqueous and organic phases, reduces the interfacial tension, and increases the diffusion rate of diamine monomers to the organic phase (Figure 5) which means an increase in the rate of diffusion enhances the IP area and generates a rougher PATFC membrane (Kwak *et al.* 2001; Kim *et al.* 2005). Membranes with higher surface roughness could result in

higher water permeation, due to a more effective surface area (Roh & Khare 2002; Huang *et al.* 2008).

Due to the ability of TMC monomer to form three-dimensional polyamide backbone structures, it was assumed that there are two types of pores in the PATFC membrane layer: network pores and aggregate pores. The small spaces between polymer backbones constituting network pores, reaction between PIP amines and TMC acyl chlorides and their cross-linking bond formed network pores in each aggregate; whereas the large spaces surrounded by polymer aggregates formed aggregate pores.

In presence of DMSO additive due to an increase in the diffusion rate of PIP into organic phase, as was reported in the literature, the diagonals and distributions of pore size of network and aggregate pores get larger as the concentration of DMSO increases. If there is a pore larger than the critical value, in a high concentration of DMSO additive,

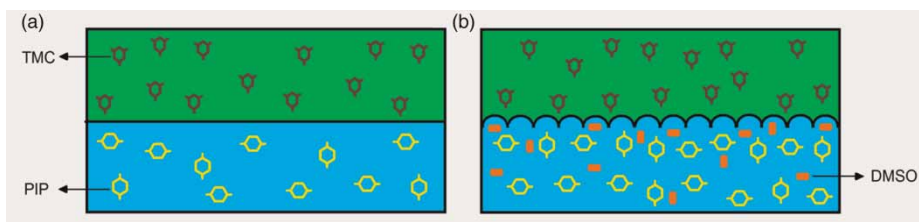


Figure 5 | Schematic for representing the effect of DMSO on the formation of surface morphology (a) without and (b) with addition of DMSO.

some direct flow of solutes occurs in pores of PATFC membrane layer. Hence, concentration of DMSO additive should be optimum until salt rejection is not lost.

The MWCO is the molecular weight of the smallest macromolecule which is rejected more than 90% by membrane. Polyethylene glycol (PEG) is used to measure the MWCO value because of a wide range in molecular weight and ineffectiveness in membrane properties. The MWCO of the polyamide membranes was evaluated with three different feed aqueous solutions of PEG (500 ppm) with molecular weights of 1,000, 2,000, and 4,000 g/mol. Figure 6 shows the MWCO values of different polyamide membranes prepared with and without DMSO as aqueous phase additive. The value of MWCO for polyamide membrane was 1,500 Da (rejection = 94.7%), which was higher than MWCO of polyamide membrane containing 6 wt% DMSO and equal to 2,000 Da (rejection = 96.3%). The average membrane pore diameter related to $MWCO = 1,380$ and $1,710$ was 1.4 and 1.7 nm, respectively (Chakrabarty *et al.* 2008). Results indicate that polyamide membrane containing DMSO additive had the largest pore size compared to the polyamide membrane without DMSO. These results are also compatible with the membrane flux presented earlier.

The changes of salt rejection of membrane in different feed solution pHs are shown in Figure 7. The pH was adjusted by addition of NaOH and HCl to the feed solution. In this case, the variations of salt rejection were apparently due to Donnan exclusion change, rather than structural changes in the surface layer. As shown in Figure 7, salt rejection of membrane changes from $R_{Na_2SO_4} > R_{NaCl} > R_{CaCl_2}$ at pH = 11 to $R_{CaCl_2} > R_{Na_2SO_4} > R_{NaCl}$ at pH = 3. The results

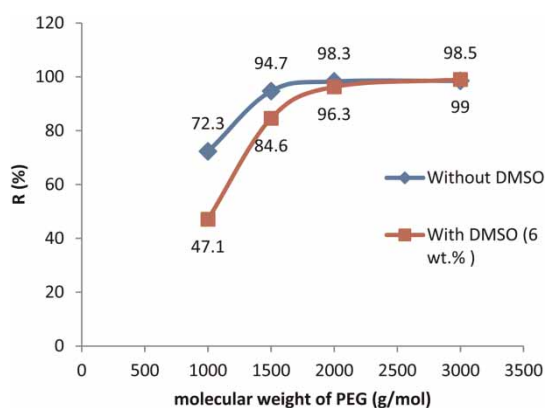


Figure 6 | Rejection of different molecular weights PEG.

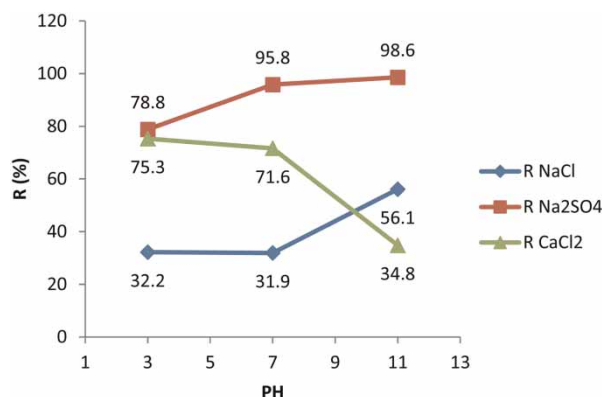


Figure 7 | Effect of feed solution pH on membrane rejection.

clearly indicate that the membrane surface charge changes from relatively negative to relatively positive by changing the pH of feed solution from basic to acidic condition. In basic environment, carboxylic acid ($-\text{COOH}$) groups in polyamide chains convert to carboxylate (COO^-) anions and therefore, the negative surface charge of membrane increases. While in acidic environment, positive surface charge increases due to conversion of amine (NR_3) groups to quaternary ammonium ($-\text{NR}_4^+$) groups.

CONCLUSION

In this study, we showed that the presence of DMSO during IP affects the performance and morphology of prepared PATFC membranes. Water and n-hexane are two immiscible phases. DMSO has a solubility parameter between water and n-hexane solutions. Hence, addition of DMSO into the aqueous phase increased the solubility of two phases. A rise in miscibility leads to an increase in mass transfer of diamines to organic phase, and subsequently an ascent in the membrane roughness and effective area. In the presence of 6% DMSO in IP reaction of PA layer on the PSF support, water permeability was increased, up to 46%, while salts rejection remained approximately constant.

REFERENCES

Abu Seman, M. N., Khayet, M. & Hilal, N. 2011 Development of antifouling properties and performance of nanofiltration

- membranes modified by interfacial polymerization. *Desalination* **273**, 36–47.
- Ahmad, A. L. & Ooi, B. S. 2006 Optimization of composite nanofiltration membrane through pH control: Application in CuSO₄ removal. *Sep. Purif. Technol.* **47**, 162–172.
- Akbari, A., Desclaux, S., Remigy, J. C. & Aptel, P. 2002 Treatment of textile dye effluents using a new nanofiltration membrane. *Desalination* **149**, 101–107.
- Akbari, A., Desclaux, S., Rouch, J. C., Aptel, P. & Remigy, J. C. 2006 New UV-photografted nanofiltration membranes for the treatment of colored textile dye effluents. *J. Membr. Sci.* **286**, 342–350.
- Belfer, S., Gilron, J., Purinson, Y., Fainshtain, R., Daltrophe, N., Priel, M., Tenzer, B. & Toma, A. 2001 Effect of surface modification in preventing fouling of commercial SWRO membranes at the Eilat seawater desalination pilot plant. *Desalination* **139**, 169–176.
- Bouranene, S., Fievet, P., Szymczyk, A., El-Hadi Samar, M. & Vidonne, A. 2008 Influence of operating conditions on the rejection of cobalt and lead ions in aqueous solutions by a nanofiltration polyamide membrane. *J. Membr. Sci.* **325**, 150–157.
- Chakrabarty, S., Purkait, M. K., Gupta, S. D., De, S. & Basu, J. K. 2003 Nanofiltration of textile plant effluent for color removal and reduction in COD. *Sep. Purif. Technol.* **31**, 141–151.
- Chakrabarty, B., Ghoshal, A. K. & Purkait, M. K. 2008 Effect of molecular weight of PEG on membrane morphology and transport properties. *J. Membr. Sci.* **309**, 209–221.
- Chiang, Y. C., Hsub, Y. Z., Ruaana, R. C., Chuang, C. J. & Tung, K. L. 2009 Nanofiltration membranes synthesized from hyperbranched polyethyleneimine. *J. Membr. Sci.* **326**, 19–26.
- Hirose, M., Ito, H. & Kamiyama, Y. 1996 Effect of skin layer surface structure on the flux behavior of RO membranes. *J. Membr. Sci.* **121**, 209–215.
- Hirose, M., Ito, H., Maeda, M. & Tanaka, K. 1997 Highly permeable composite reverse osmosis membrane, method of producing the same, and method of using the same. US Patent 5, 614, 099.
- Huang, S. J., Hsu, C. J., Liaw, D. J., Hu, C. C., Lee, K. R. & Lai, J. Y. 2008 Effect of chemical structures of amines on physicochemical properties of active layers and dehydration of isopropanol through interfacially polymerized thin-film composite membranes. *J. Membr. Sci.* **307**, 73–81.
- Jahanshahi, M., Rahimpour, A. & Peyravi, M. 2010 Developing thin film composite poly(piperazine-amide) and poly(vinyl-alcohol) nanofiltration membranes. *Desalination* **257**, 129–136.
- Kim, S. H., Kwak, E. Y. & Suzuki, T. 2005 Positron annihilation spectroscopic evidence to demonstrate the flux-enhancement mechanism in morphology-controlled thin-film-composite (TFC) membrane. *Environ. Sci. Technol.* **39**, 1764–1770.
- Korikov, A. P., Kosaraju, P. B. & Sirkar, K. K. 2006 Interfacially polymerized hydrophilic microporous thin film composite membranes on porous polypropylene hollow fibers and flat films. *J. Membr. Sci.* **279**, 588–600.
- Kwak, S. Y., Jung, S. G. & Kim, S. H. 2001 Structure-motion-performance relationship of flux-enhanced reverse osmosis (RO) membranes composed of aromatic polyamide thin films. *Environ. Sci. Technol.* **35**, 4334–4340.
- Lopes, C. N., Carlos, J., Petrus, C. & Riella, H. G. 2005 Color and COD retention by nanofiltration membranes. *Desalination* **172**, 77–83.
- Manttari, M., Viitikko, K. & Nystrom, M. 2006 Nanofiltration of biologically treated effluents from the pulp and paper industry. *J. Membr. Sci.* **272**, 152–160.
- Mukherjee, D., Kulkarni, A. & Gill, W. N. 1994 Flux enhancement of reverse osmosis membranes by chemical surface modification. *J. Membr. Sci.* **97**, 231–249.
- Mulder, M. 1996 *Basic Principles of Membrane Technology*. Kluwer Academic Publishers, Dordrecht.
- Petersen, R. J. 1993 Composite reverse osmosis and nanofiltration membranes. *J. Membr. Sci.* **83**, 81–150.
- Puro, L., Manttari, M., Pihlajamaki, A. & Nystrom, M. 2006 Characterization of modified nanofiltration membranes by octanoic acid permeation and FTIR analysis. *Chem. Eng. Res. Design* **84**, 87–96.
- Rahimpour, A., Jahanshahi, M., Mortazavian, N., Madaeni, S. S. & Mansourpanah, Y. 2010 Preparation and characterization of asymmetric polyethersulfone and thin-film composite polyamide nanofiltration membranes for water softening. *Appl. Surf. Sci.* **256**, 1657–1663.
- Roh, I. J. & Khare, V. P. 2002 Investigation of the specific role of chemical structure on the material and permeation properties of ultrathin aromatic polyamides. *J. Mater. Chem.* **12**, 2334–2338.
- Singh, P. S., Joshi, S. V., Trivedi, J. J., Devmurari, C. V., Prakash Rao, A. & Ghosh, P. K. 2006 Probing the structural variations of thin film composite RO membranes obtained by coating polyamide over polysulfone membranes of different pore dimensions. *J. Membr. Sci.* **278**, 19–25.
- Uyak, V., Koyuncu, I., Oktem, I., Cakmakci, M. & Toroz, I. 2008 Removal of trihalomethanes from drinking water by nanofiltration membranes. *J. Hazard. Mater.* **152**, 789–794.
- Verissimo, S., Peinemann, K. V. & Bordado, J. 2006 Influence of the diamine structure on the nanofiltration performance, surface morphology and surface charge of the composite polyamide membranes. *J. Membr. Sci.* **279**, 266–275.
- Wei, X. Z., Zhu, L. P., Deng, H. Y., Xu, Y. Y., Zhu, B. K. & Huang, Z. M. 2008 New type of nanofiltration membrane based on crosslinked hyperbranched polymers. *J. Membr. Sci.* **323**, 278–287.
- Zhang, Y., Xiao, C., Liu, E., Du, Q., Wang, X. & Yu, H. 2006 Investigations on the structures and performances of a polypiperazine amide/polysulfone composite membrane. *Desalination* **191**, 291–295.